# Investigation of the Olive Mill Solid Wastes Pellets Combustion in a Counter-Current Fixed Bed Reactor

**Mohamed Ali Mami [1], Hartmut Mätzing [2], Hans-Joachim Gehrmann [2], Dieter Stapf [2], Rainer Bolduan [3] and Marzouk Lajili [1,\*]**

[1] Ionized and Reactive Media Studies Research Unit (EMIR), Preparatory Institute of Engineering Studies of Monastir (IPEIM), University of Monastir, 15 Avenue Ibn El Jazar Monastir 5019, Tunisia; Mohamedali.Mami@ipeim.rnu.tn

[2] Institute for Technical Chemistry (ITC), Karlsruhe Institute of Technology (KIT), Hermann-von-Helmholtz-Platz 1, 76344 Eggenstein-Leopoldshafen, Germany; hartmut.maetzing@kit.edu (H.M.); hans-joachim.gehrmann@kit.edu (H.-J.G.); dieter.stapf@kit.edu (D.S.)

[3] European Institute for Energy Research (EIFER), Karlsruhe Institute of Technology (KIT), Emmy-Noether-Str. 11, 76131 Karlsruhe, Germany; Rainer.Bolduan@eifer.uni-karlsruhe.de

[\*] Correspondence: marzouk.lajili@ipeim.rnu.tn; Tel.: +216-73500277 or +216-97369126

**Abstract:** Combustion tests and gaseous emissions of olive mill solid wastes pellets (olive pomace (OP), and olive pits ($OP_i$)) were carried out in an updraft counter-current fixed bed reactor. Along the combustion chamber axis and under a constant primary air flow rate, the bed temperatures and the mass loss rate were measured as functions of time. Moreover, the gas mixture components such as $O_2$, organic carbon ($C_{org}$), $CO$, $CO_2$, $H_2O$, $H_2$, $SO_2$, and $NO_x$ ($NO + NO_2$) were analyzed and measured. The reaction front positions were determined as well as the ignition rate and the reaction front velocity. We have found that the exhaust gases are emitted in acceptable concentrations compared to the combustion of standard wood pellets reported in the literature (EN 303-5). It is shown that the bed temperature increased from the ambient value to a maximum value ranging from 750 to 1000 °C as previously reported in the literature. The results demonstrate the promise of using olive mill solid waste pellets as an alternative biofuel for heat and/or electricity production.

**Keywords:** olive mill solid wastes (OMSWs); fixed bed combustor; pellets; combustion parameters; gaseous emissions

## 1. Introduction

Agro-industrial by-products are viable alternatives to fossil fuels to reduce greenhouse gases emissions such as $CO_2$ and $NO_x$ [1–3]. Among these by-products, olive mill solid wastes (OMSWs) are generated in large quantities in the leading producers in the olive oil industry, including Spain, Italy, Greece, and Tunisia. However, these by-products can present serious environmental problems affecting soil, air, and water when stockpiled and left untreated. However, these lignocellulosic biomasses can be considered as a promising source of renewable energy [4,5]. Indeed, these residues can be separated as olive pomace (OP) and olive pits ($OP_i$). Olive pits ($OP_i$) are a major bio-fuel in Spain [6], which is used in combustion processes to produce heat [7] owing to its low moisture content, high heating value, uniform size, and relatively high bulk density [8]. Using this material as a biofuel can be considered as an economically viable alternative to fossil fuels [9]. Despite this potential, only a few studies have been dedicated to characterizing this biofuel for the purpose of energy conversion [5]. Nevertheless, the value of the utilization of olive pomace as a biofuel is widely recognized [10,11]. Moreover, both OP and $OP_i$ can be processed into cylindrical pellets (up to 40 mm length, at standard diameter from 6 to 10 mm, typically 6 mm). This process increases the energy density of these pellets [12,13].

Although the pelletization is a very complicated technique, with the potential for technical problems to arise, we concluded that when using the olive mill solid wastes with moisture content in the vicinity of 15%, and at the optimal conditions of frequency and temperature as we mention below, no problems will be encountered. The reason for this is that the lignocellulosic biomass contains its own binder (abrasive matter). However, it should be mentioned that in the case of this study, pelletization was successful without any additive binder and with the appropriate individual die. The samples of about 1 mm in size needed neither milling nor moisture adjustment and could directly be pelletized after homogenization.

The combustion behavior of pellets, either mixed with other residues or only derived from the OMSWs, has been studied in small powered pellets boilers (<50 kW). These investigations have shown that olive solid residue pellets are ecologically beneficial and are an environmentally friendly energy source for producing heat and/or electricity [14–16]. Nevertheless, the combustion of such biofuels in fixed/fluidized beds is rarely reported in the literature. Moreover, these high calorific pellets have not been commonly used in large-scale combustion systems. Indeed, except for the high quality woody pellets like DIN-plus which is commercialized in European markets, pellets like those considered in our work have not yet been investigated which may be because of the additional cost of transport and pelletization. For this reason, countries like Spain and Italy are still using raw olive mill by-products which have been dried and exhausted without pelletization. However, the pelletization has proven to be very suitable for heat production (domestic use for household boilers and stoves) [14,15]. Due to the higher ash volume ($\approx$5%) of olive residues in comparison with woody biomass for DIN plus (<1%) filtering/ash management/burner suitability, as well as standardized industrial pellet requirement, must be considered for large-scale application. Further, their combustion produces more emissions than high quality woody pellets.

González et al. [14] have studied the combustion of different pellets made from olive stones ($OP_i$), tomato residues, and cardoon, respectively, in a mural boiler used for domestic heating (11.6 kW). The results were compared with forest wood pellets which are recommended as standard fuels. The authors showed that when using $OP_i$ pellets, characterized by lower percentages of sulfur and nitrogen contents, they obtained a significant decrease in $NO_x$ and $SO_2$ emissions. These biofuels represented the most favorable and attractive fuels from an environmental point of view by comparison to the tomato, cardoon, and forest wood pellets.

In the same context, Miranda et al. [17] conducted combustion tests on OMSWs ($OP_i$ and OP) in their raw state (not pelletized). They used a prototype furnace to analyze the main combustion emissions: $CO$, $CO_2$, $NO_x$, $N_2O$, $SO_2$, and $O_2$. The tests resulted in a good combustion efficiency with relatively low emissions.

Several groups are currently focusing on the modeling of the combustion of pellets in reactors such as pilot fixed bed/fluidized bed, before expanding these studies to large scales (industrial plants) [18]. The choice of the fixed bed reactor for our study is based on its relative simplicity, which will be easier to eventually model. At the same time, our study allows the determination of the independent characteristic numbers needed to scale our results to an industrial scale [19–21].

To the best of our knowledge, the combustion of olive solid residues, such as OP and $OP_i$, in a counter-current fixed bed reactor has not been reported in the literature. In this study, the combustion pellets tests were carried out in the 40 kW fixed bed reactor "KLEAA" at Karlsruhe Institute of Technology (KIT) (Germany) [22,23]. To determine the combustion characteristics of these samples, the axial temperature evolution was measured. This permits the determination of the reaction front positions in terms of time during the combustion process. In addition, the mass loss is continuously measured during the test. Further, gaseous emission such as $CO$, $CO_2$, $H_2$, $H_2O$, $O_2$, and organic carbon ($C_{org}$) were analyzed and measured as well as other pollutants: $SO_2$ and $NO_x$ ($NO + NO_2$). Consequently, some scale independent characteristic numbers such as the reaction front velocity $u_{RF}$, the ignition rate (*IR*), the mass conversion rate (*MCR*) and the specific heat release rate (*HR*) were derived. These specific numbers can serve to quantify and to assess the combustion quality.

All obtained results are compared to those of similar studies in literature and to standard wood pellets (EN-303-5).

## 2. Materials and Methods

### 2.1. Samples Preparation

Olive pomace (OP) and olive pits (OP$_i$) used in this study were obtained from the Zouila Oil Press Company located in the Sahel region of Tunisia (Mahdia-Tunisia). About 6 kg of pellets were prepared from the biofuels at EIFER (European Institute for Energy Research, Karlsruhe, Germany): 100% OP with a die compaction rate of 1:5 (conical pressing) and 100% OP$_i$ with a compaction rate of 1:4 at 24 mm press channel length for both. The pellet press used is a Kahl lab scale flat matrix press 14–175 (with a maximum olive pellet production in the range 15–20 kg/h). The specific optimum rotation frequency was determined to be 85 Hz, and the optimum temperature for stable pellets in literature was 75 °C. The produced pellets were in compliance with the German and European standards (EN 303-5, EN 17225-6). After pelletization and air-cooling, the pellets were stored for minimum 24 h under room conditions to equalize any moisture differences as shown in Table 1.

**Table 1.** Operating pelletization condition.

| Pelletizer Performance | 100% Olive Pomace (OP) | 100% Olive Pits (OP$_i$) |
|---|---|---|
| Pelletizing temperature (°C) | 60 | 51 |
| Biomass moisture (% w.b.) | 14.7 ± 0.5 | 15.3 ± 0.3 |
| Pellet moisture (% w.b.) | 12.4 ± 0.4 | 13.7 ± 0.2 |

(% w.b. is the percentage on wet basis).

Table 1 indicates that the moisture content decreases after pelletization. This decrease is due to the evaporation associated with the rising temperature during the pelletization process. Finally, the obtained products were moisture-balanced cylindrical pellets of 6 mm diameter and 20–30 mm in length. As it is notable, the two OMSWs were pelletized under two different temperatures 60 and 51 °C for OP and OP$_i$, respectively. Indeed, because of its oil content and lubricity, pelletizing of olive pomace caused higher resistance (see compaction rate), and the higher friction, subsequently, raised the temperature to evaporate more water than during olive pits pelletizing. Hence, final moisture contents should be different because pelletization started with different initial moistures under different temperatures and calculations were done on wet basis. It can be observed that the difference between final moisture content on wet basis does not exceed 1.3%. Thereby, even though the moisture directly affects the low heating value (*LHV*), the difference between the two fuel types will be small.

### 2.2. Samples Characterizations

#### 2.2.1. Raw Samples Characterizations

Ultimate and proximate analysis of the raw samples as olive pomace (OP), olive pits (OP$_i$) and sawdust (S) are summarized in Table 2.

Tables 2 and 3 show the ultimate and proximate analyses and the energy characteristics of the used raw materials. These characteristics are compared with those found in the literature for different agro-industrial wastes. All analyses were carried out at the Chemical and Microbiological Institute UEG GmbH (Germany). Ultimate, proximate and energy contents were realized according to the standards analytical methods for solid fuels. High heating value (*HHV*) is measured using a calorimetric bomb, and the *LHV* is then calculated using:

$$LHV = HHV - L_v \left( \frac{9\% \, \mathrm{H} + \% \, M}{100} \right) \tag{1}$$

where, *LHV* is the low heating value, *HHV* is the high heating value, % H is the hydrogen content and % *M* is the moisture content.

The energy density (*ED*) is obtained when multiplying the bulk density $\rho_{BD}$ by the *LHV*:

$$ED = \rho_{BD} \times LHV \tag{2}$$

where, *ED* is the energy density and $\rho_{BD}$ is the bulk density.

**Table 2.** Raw materials characteristics.

| Samples | Equivalent Formula d.b.a.f. [a] | Ultimate Analysis (% d.b.) | | | | | Proximate Analysis (% d.b.) | | |
|---|---|---|---|---|---|---|---|---|---|
| | | % C | % H | % O | % N | % S | % ash | % FC | % VM |
| Olive pomace (OP) | $CH_{1.54}O_{0.56}N_{0.024}$ | $52.2 \pm 0.8$ | $6.70 \pm 0.3$ | $39.6 \pm 0.6$ | $1.50 \pm 0.1$ | $0.08 \pm 0.01$ | $5.10 \pm 0.10$ | $18.90 * \pm 0.3$ | $76.0 \pm 1.0$ |
| Olive pits ($OP_i$) | $CH_{1.97}O_{0.92}N_{0.018}$ | $41.4 \pm 0.4$ | $5.20 \pm 0.2$ | $52.5 \pm 0.9$ | $0.91 \pm 0.1$ | $<0.2$ | $0.80 \pm 0.1$ | $15.20 * \pm 0.2$ | $84.0 \pm 0.8$ |
| Sawdust (S) | $CH_{1.49}O_{0.6}N_{0.0035}$ | $51.5 \pm 0.5$ | $6.40 \pm 0.3$ | $41.9 \pm 0.5$ | $0.20 \pm 0.1$ | $<0.1$ | $0.5 \pm 0.1$ | $24.50 * \pm 0.10$ | $75.0 \pm 1.0$ |
| Spruce wood [24,25] | $CH_{1.41}O_{0.59}N_{0.0033}$ | 51.9 | 6.10 | 40.9 | 0.30 | 0.30 | 1.70 | 18.10 | 80.2 |
| Wood [26,27] | $CH_{1.46}O_{0.6}N_{0.0016}$ | 51.6 | 6.3 [b] | 41.5 | 0.10 | 0.10 [b] | 1.0 | 17.0 | 82.0 |
| Palm Kernels [3,27] | $CH_{1.52}O_{0.58}N_{0.038}$ | 51.0 | 6.50 | 39.5 | 2.30 | 0.27 | 5.20 | 17.50 | 77.30 |
| OP (Turkish) [28] | $CH_{1.36}O_{0.53}N_{0.021}$ | 51.3 | 5.85 | 36.9 | 1.27 | 0.08 | 4.51 | 17.90 | 71.17 |
| OP (Italy) [29] | $CH_{1.57}O_{0.91}N_{0.034}$ | 44.2 | 5.80 | 48.2 | 1.80 | - | 5.40 | 29.60 | 65.0 |
| $OP_i$ (Spain) [17] | $CH_{1.71}O_{0.57}N_{0.0009}$ | 52.2 | 7.48 | 40.0 | 0.06 | $<0.1$ | 0.56 | 18.50 | 80.94 |
| $OP_i$ (Spain) [30] | $CH_{1.6}O_{0.82}N_{0.0019}$ | 44.8 | 6.0 | 49.1 | 0.10 | 0.01 | 1.40 | 13.80 | 74.40 |

% d.b. is the percentage on dry basis; * Calculated by difference: % O = 100 − (% H + % C + % N), % FC = 100 − (% ash + % VM), [a] dry basis ash free, [b] Average value, - Not determined.

**Table 3.** Energy contents in the raw materials.

| Samples | *LHV* (MJ/kg) | $\rho_{BD}$ $(kg/m^3)$ | *ED* $(GJ/m^3)$ |
|---|---|---|---|
| Olive pomace (OP) | $17.90 \pm 0.40$ | $539 \pm 10$ | $9.60 \pm 0.50$ |
| Olive pits ($OP_i$) | $17.29 \pm 0.20$ | $764 \pm 12$ | $13.20 \pm 0.36$ |
| Sawdust (S) | $16.30 \pm 0.10$ | $103 \pm 3$ | $1.60 \pm 0.06$ |
| Spruce wood [24,25] | 18.10 | 105 | 1.90 |
| Palm Kernels [26,27] | 17.00 | 500 | 8.50 |
| OC (Turkish) [31] | 19.60 | 591 | 11.58 |
| OC (Jordan) [32] | 23.056 | 558 | 12.86 |
| $OP_i$ (Spain) [8] | 14.70 ** | 651.90 ** | 9.85 |
| Oke (Greece) [33] | 19.36 | 573 | 11.09 |
| Rice Husks [34] | 14.90 | 200 | 2.820 |

OC: Olive cake, Oke: Olive kernels, ** As received.

Furthermore, Table 2 shows high Nitrogen contents for OP and $OP_i$ in comparison with the sawdust (0.2%) and wood (0.1%). This fact will explain why nitrogen oxide emissions were relatively high.

As can be seen from Table 2, the ash content in the two samples (OP and $OP_i$) is high (3% and 4.7%) compared with 0.5% value for sawdust. For the two samples, the Energy density is higher than many biomass types in Table 3. Hence, the pelletization process is a compulsory process to increase the energy density of pellets and to make their transport and storage easier, ensuring a high hardness and long durability [35,36].

2.2.2. Pellets Samples Characterizations

Two pellets samples types were prepared: 100% olive pomace (OP) and 100% olive pits ($OP_i$). It needs to be clarified that the number of pellets used depends on the nature of characterization test we realize. For example, in the case of measuring the average length, diameter, and unit density (mass of the pellet divided by its volume) at least a 100 pellets are required to decrease the error according to the central limit theorem ($\varepsilon \sim \frac{1}{\sqrt{N}}$), where $\varepsilon$ is the error and N is the number of samples. For the bulk density determination, the volume of the container (100 cm³ in our case) ensured a large number of pellets was achieved. For the moisture content determination, the volume of the stove allowed a maximum of 10 crucibles containing one 1 pellet each to be used. The same process was undertaken when determining the ash content with a muffle furnace. However, for measuring the *HHV* via a calometric bomb, we used about 1 g of pellet and we repeated the test 5 times to attain the average

value (this test is delicate and costly). In addition, during the pyrolysis tests to determine the volatile matter in a thermogravimetric balance, tests were repeated 3 times because this test type is time and cost intensive. Nevertheless, it was found that relative uncertainties were smaller than 5% of the mean value.

The main chemical characteristics of the produced pellets based on ultimate and proximate analysis are summarized in Table 4. These analyses are compared to the standard wood pellets and to other pellets presented in the literature. We observe that our prepared pellets show typical compositions when compared to other biomasses available in the literature [16,17,37].

The ash content was determined using a muffle furnace for which the temperature was fixed at 815 °C. The resulting values were lower than those fixed by the European normalization (<5%). In addition, the nitrogen content was 1.26% for OP and 0.61% for $OP_i$, respectively. These values were relatively higher than 0.11% obtained for wood pellets. The sulphur content was <0.1% for both samples. Therefore, $SO_x$ emissions are expected to be insignificant.

**Table 4.** Pellets characteristics.

| Samples | Equivalent Formula d.b.a.f. | Ultimate Analysis (% d.b.) | | | | | Proximate Analysis (% d.b.) | | |
|---|---|---|---|---|---|---|---|---|---|
| | | % C | % H | % O | % N | % S | % ash | % FC | % VM |
| 100% OP | $CH_{1.3}O_{0.57}N_{0.021}$ | 49.50 ± 0.50 | 5.4 ± 0.5 | 43.70 * ± 1.80 | 1.3 ± 0.6 | <0.10 | 2.90 ± 0.10 | 17.70 * ± 0.10 | 79.40 ± 0.20 |
| 100% $OP_i$ | $CH_{1.65}O_{0.74}N_{0.011}$ | 46.50 ± 0.80 | 6.3 ± 0.1 | 46.60 * ± 0.90 | 0.5 ± 0.1 | <0.10 | 1.90 ± 0.10 | 15.70 * ± 0.20 | 82.40 ± 1.00 |
| wood pellets | $CH_{1.4}O_{0.63}N_{0.002}$ | 46.30 ± 0.20 | 5.4 ± 0.2 | 48.19 * ± 1.00 | 0.11 | <0.10 | 0.30 ± 0.02 | 24.30 ± 0.90 | 75.40 ± 0.70 |
| OP (Spain) [16] | $CH_{1.52}O_{0.49}N_{0.032}$ | 54.75 | 6.17 | 37.00 | 1.98 | <0.10 | 5.55 | 17.28 | 77.17 |
| OP (Spain) [17] | $CH_{1.65}O_{0.47}N_{0.007}$ | 58.20 | 6.00 | 35.40 | 0.40 | 0 | 2.50 | 17.69 | 79.81 |

* Calculated by difference.

In Table 5 the *LHV* values range between 17.45 and 20.36 MJ/kg. The energy density values of our samples were reasonably good (14.42 GJ/$m^3$ for $OP_i$ and 15.59 GJ/$m^3$ for OP). However, the effect of pelletization was much more notable with OP than with $OP_i$. This is because of the difference in the bulk density between the two raw materials attributable to the better compressibility of the pomace (along with higher pressing energy needs) compared to the pits. On the other hand, the durability (*Du*), which is determined as a function of the percentage of fine particles leaving the pellets after appropriate mechanical tests, showed acceptable percentages with high regression factor ($R^2$ = 0.985) [38]. Indeed, after pelletization the pellets can be stored for longer before its use. During this period fine particles can leave the pellets so that the mass and, thereby, the energy of the fuel decreases. By using a centrifugation system based in a gyratory motor under standard normalizations (ISO 17831-1), the mechanical durability can be determined by weighing the mass before starting the experiment and subsequently. Thereafter, a percentage of material which is remaining in the fuel can be calculated: This is the so-called durability. The durability provides a reasonable assessment in regard to the transport and storage of a given solid biofuel [39]. Values of durability for both prepared samples (OP and $OP_i$) were in the same range of standard wood pellets. In addition, obtained durability (88–89%) for the peanut hull pellets agreed with our results [38].

**Table 5.** Energy contents in the pellets samples.

| Samples | *LHV* (MJ/kg) | $\rho_{BD}$ $(kg/m^3)$ | *ED* (GJ/$m^3$) | *Du* (% w.b.) |
|---|---|---|---|---|
| OP pellets | 19.02 ± 0.40 | 820 ± 15 | 15.59 ± 0.62 | 88 ± 2 |
| $OP_i$ pellets | 18.38 ± 0.10 | 785 ± 10 | 14.42 ± 0.25 | 85 ± 2 |
| wood pellets | 17.45 ± 0.30 | 660 ± 8 | 11.51 ± 0.33 | 89 ± 2 |
| OP (Spain) [16] | 20.36 | 780 | 15.80 | - |
| OP (Tunisia) [37] | 19.23 | 920 | 17.69 | - |

## 3. Combustion Test

The experimental studies were carried out in a batch fixed bed reactor (KLEAA) characterized by a nominal power of 40 kW. This device is located at the Institute for Technical Chemistry (ITC) at the Karlsruhe Institute of Technology (KIT) in Germany.

The counter-current fixed bed reactor KLEAA has three main components: The combustion chamber composed by a fixed bed and a heated furnace, the post (or secondary) combustion chamber, and the flue gas cleaning system, which is equipped with a heat exchanger, a bag filter, and a carbon absorber.

The facility is suited to perform limited tests of solid fuel samples (about 3 kg for each test). The fuel bed has a total volume of 10 L. The furnace, and the secondary combustion chamber can be heated electrically up to a temperature of 1100 °C. The major components of the installation are represented schematically in Figure 1. A more detailed description of the facility is available elsewhere [21–23].
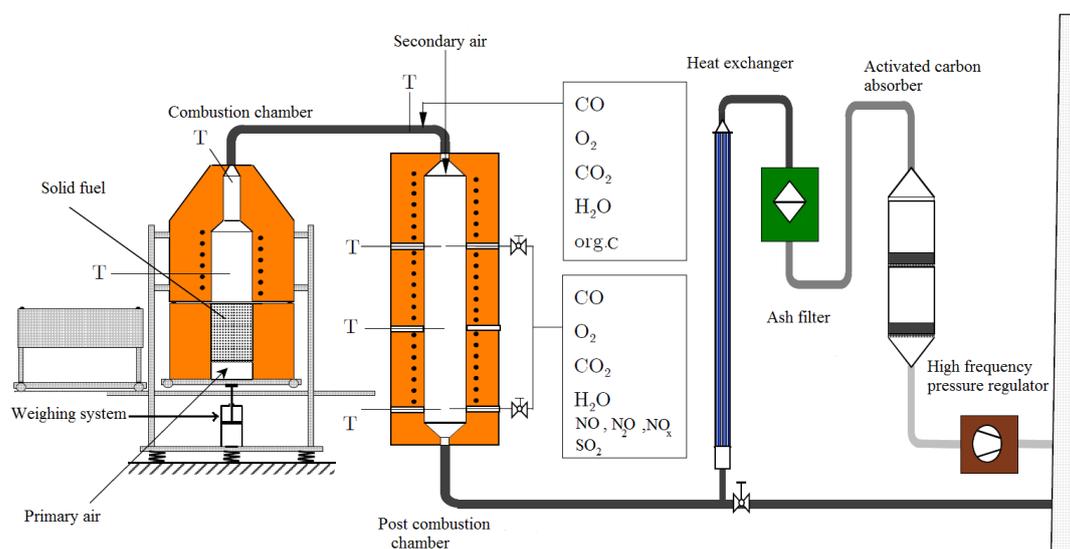


**Figure 1.** Sketch of the counter-current fixed bed reactor (KLEAA) facility at ITC, Karlsruhe, Germany.

The fixed bed has a height, h, of 250 mm and a diameter, d, of 230 mm. It is equipped with thirteen K-type thermocouples which are arranged in 20 mm intervals along the chamber's axis to measure the central bed temperature as it is shown in Figure 2.
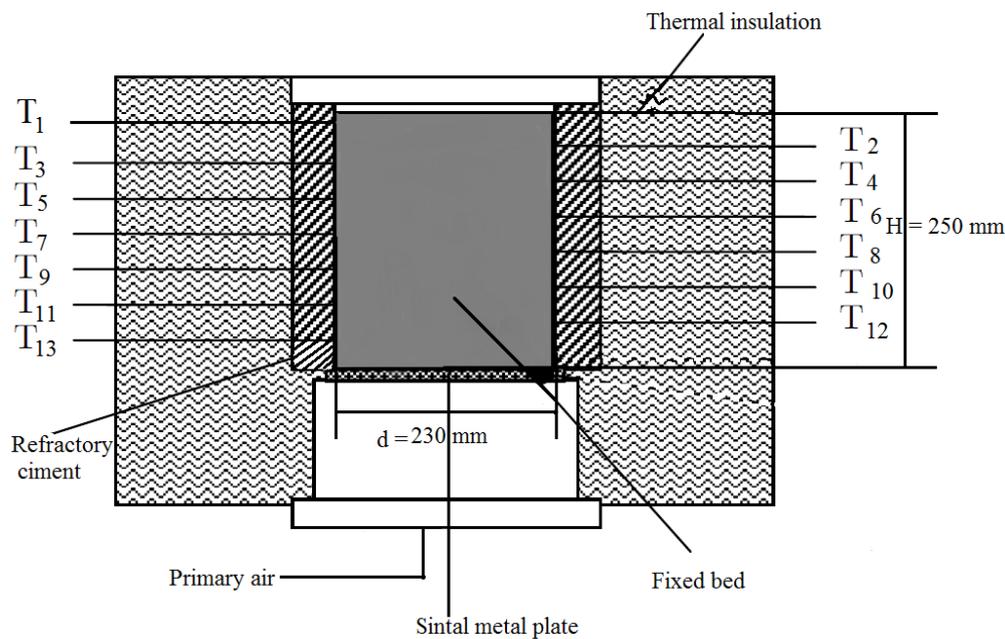
**Figure 2.** The fixed bed reactor and the thermocouples disposition.

Two experimental tests were performed with the biofuel pellets:

- 3.5 kg of 100% olive pomace (OP).
- 3.75 kg of 100% olive pits (OP$_i$).

The pellet samples were introduced into the combustion chamber. Then, the pellet samples were moved to the hot furnace, so that the fixed bed will be heated by radiation from the hot furnace wall (900 °C). The primary air was supplied at the bottom of the fixed bed via a sintered metal plate. The flow rate of the primary air was fixed at 10 Nm$^3$/h. The temperatures of the primary and the secondary air (25 Nm$^3$/h) were about 25 °C. Gaseous emissions were analyzed based on physical phenomena. Respectively CO, CO$_2$, and H$_2$O were analyzed by infrared techniques, $C_{org}$ by flame ionization detector, O$_2$ by a paramagnetic system, and H$_2$ by heat conductivity. Trace gases, such as NO, NO$_x$, N$_2$O, and SO$_2$ were followed and also measured at the outlet of the post-combustion chamber. Thus, CO$_2$, CO, H$_2$O, and SO$_2$ were measured at the outlet of the post-combustion chamber. A heat exchanger has served for the heating of the water recovery system. After the combustion, the fly ash was emitted and collected in a special box under the grate via an ash filter. A pressure regulator ensured a pressure drop across the plant of about 50 Pa.

As stated earlier, there are limited studies on the types of biofuels in this study. Therefore, our results are compared to the results of some previous experiments conducted with conventional wood pellets under almost similar conditions [21–23,40,41].

## 4. Results and Discussion

### 4.1. Temperature Evolution in the Fuel Bed

Figure 3 shows the evolution of the bed temperature as a function of time at various bed heights from the bottom during the combustion process of olive pomace (OP), olive pits (OP$_i$), and the standard wood pellets. The thermocouple-based temperature measurements were collected at time intervals of 5 s.

Starting from the bed top to the bottom, the temperature profiles of the pellets samples show three distinct stages: (1) the ignition delay time, (2) the main combustion phase, and (3) the final char combustion.

During the ignition delay time, the bed surface is heated slowly. Hence, it dries and ignites by the radiation heat coming from the hot furnace wall. Then the ignition front propagates from the top of the bed downwards opposite to the gas flow [42]. The ignition delay time was measured by thermocouples $T_2$ and/or $T_3$ (blue and pink). It was determined to be equal to 3.5 min, 3.2 min, and 5.1 min, respectively (Figures 3 and 4).
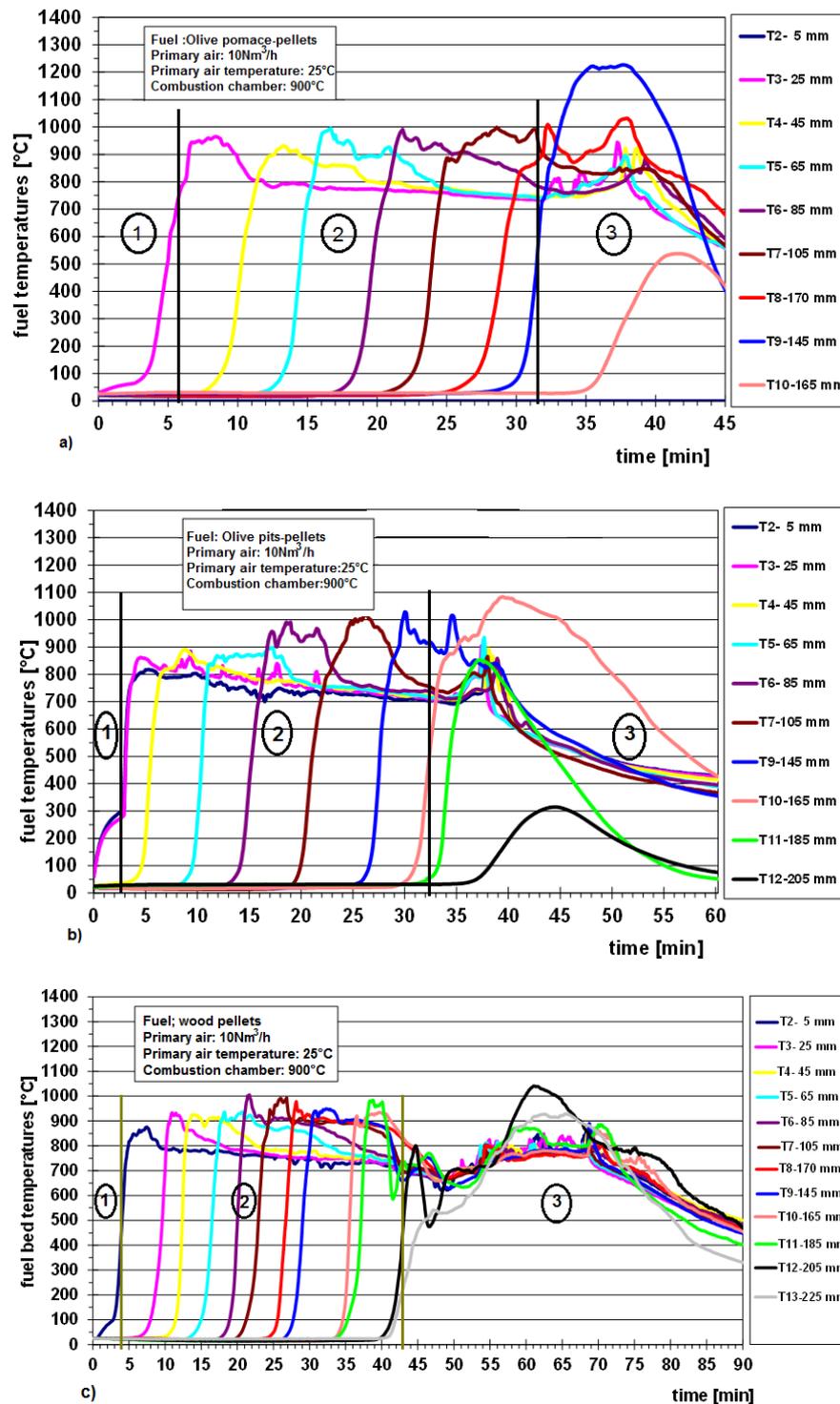


**Figure 3.** Thermocouples' readings during the passage of the flame front. (**a**) 100% olive pomace (OP); (**b**) 100% olive pits; (**c**) standard biofuel wood pellets.
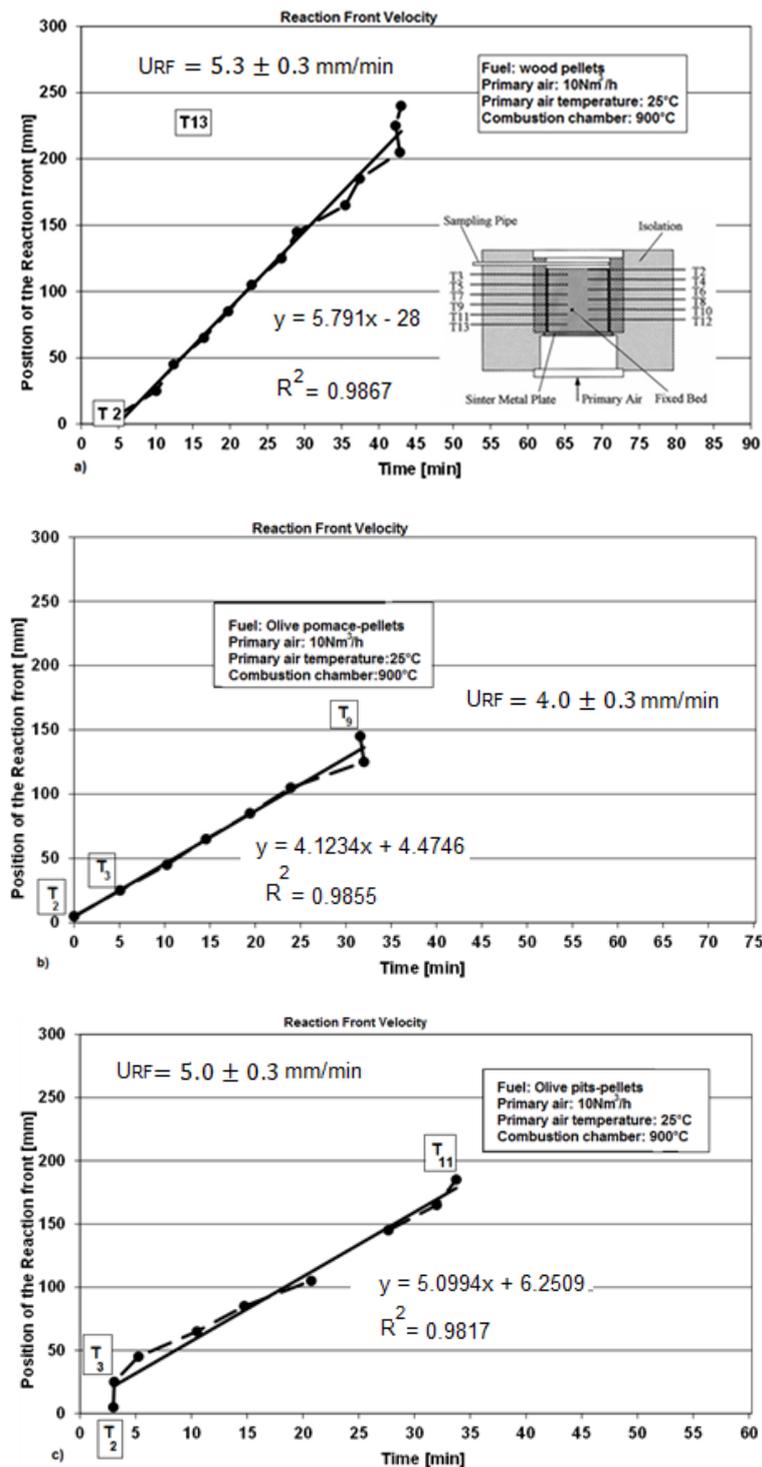
**Figure 4.** Reaction front positions derived from experimental pellets tests: (**a**) standard wood pellets; (**b**) 100% olive pomace (OP); (**c**) 100% olive pits (OP$_i$). Experimental conditions: Primary air 10 Nm$^3$/h; primary air temperature 25 °C and combustion chamber temperature 900 °C.

Thereafter, the main combustion phase starts when the flame front reaches and passes the thermocouples successively, and the temperature increases rapidly from ambient to almost 1000 °C. We observed that the temperatures rise from the initial values (25–30 °C) to reach about 880 °C for wood pellets, 800–875 °C for OP$_i$, and approximately 975 °C for OP. The observed overshoots of temperature can be explained by the highly exothermic combustion of a small amount of carbon

(coke). The arrival time and the position of the reaction front are derived from the inflection point of the temperature curves. After the passage of the reaction front, the thermocouples recorded the temperature of the hot combustion gas.

For the time interval between 30 min and 45 min (Figures 3 and 4), the reaction front reaches the bottom of the bed, and the fuel bed temperature rises again due to the heat generated by the residual char oxidation with air ($T_9$, $T_{10}$, $T_{12}$, and $T_{13}$). In this stage, some of the thermocouples may have lower temperatures than others. This resulted in a faster convective cooling [43]. A second difference appears in the maximum value of the temperature, especially during the residual carbon combustion. The OP generated a higher flame front temperature reaching 1200 °C by comparison with 1090 °C and 1050 °C for the $OP_i$ and the wood pellets, respectively. The high temperature observed in the case of olive pomace pellets can be attributed to its high heating value (22.03 MJ/kg on a dry basis). Indeed, this characteristic is strongly related to the carbon content in this sample type (49.5%) [37,44], by comparison with the 46.5% carbon content and 19.4 MJ/kg (*HHV* on a dry basis) for $OP_i$ [14], and also to the 46.3% carbon content and 18.5 MJ/kg (on a dry basis) for the wood pellets [45].

During the main combustion phase characterized by the combustion of the pyrolysis gases, no effect on heat release is observed. Thus, the temperatures profiles are quite similar for the different biofuel pellets. However, during the burning of char, the heat release (*HR*) appears quite different due to different amounts of residual carbon (Table 6). Consequently, the maximum of temperature differs significantly for each sample.

### 4.2. Mass Loss History in the Fuel Bed and Reaction Front Velocity

Further analysis of experimental results leads to the determination of some combustion parameters, such as:

The reaction front velocity:

$$u_{RF} = \frac{dh}{dt} \tag{3}$$

where $u_{RF}$ is the reaction front velocity, h is the bed height, and dt is the time increment.

The mass conversion rate:

$$MCR = \frac{\dot{m}}{A(1 - Y_{ash})} \tag{4}$$

where *MCR* is the mass conversion rate, $\dot{m}$ is the mass loss rate, *A* is the fuel bed cross section, and $Y_{ash}$ is the ash mass fraction.

The ignition rate:

$$IR = u_{RF} \times \rho_{BD} \tag{5}$$

*IR* is the ignition rate, and other variables are defined in the above equations.

The specific heat release rate:

$$HR = MCR \times HHV \tag{6}$$

where *HR* is the heat release, and the two other variables are defined in the above equations.

These characteristic numbers are useful to predict and understand quantitatively the combustion process in the fixed bed. Moreover, these parameters are independent and good indicators of the combustion behavior in large industrial facilities. They are determined in similar ways as described in the literature [22,23,46–48].

### 4.2.1. Reaction Front Velocity

The position of the reaction front is obtained based on the inflection point in the temperature profiles shown above. In Figure 4a–c, the reaction front position is plotted as a function of the elapsed time, and almost linear curves are obtained. This result indicates a steady and uniform propagation of the flame front. For both samples (OP and $OP_i$), the reaction front velocities were equal to 3.50 mm/min and 4.00 mm/min respectively (Figure 4b,c); whereas, in the case of wood pellets the

reaction front velocity is almost 4.40 mm/min (Figure 4a). The regression factor ($R^2$) exceeds 0.90 for all reported regressions.

### 4.2.2. Mass Loss History

The mass conversion rate (*MCR*) is defined as the mass loss per unit area and per unit time. It is obtained directly from the measured mass of the fixed bed, and thereafter, corrected by considering the ash content of the fuel.

The ignition rate (*IR*) defines the quantity of fuel ignited per unit area and per unit time due to the reaction front. This ignition rate is a crucial parameter used to estimate the grate position, where the reaction front reaches its limit at the bottom of the bed, indicating the end of the fuel combustion. Moreover, the heat release rate (*HR*) is determined by multiplying the *HHV* value and the mass conversion rate (Equation (6)).

However, the specific heat release in the main combustion zone (*HR I*) is calculated using *MCR I* and the *HHV* of the fuel. In the char residual oxidation phase, this value (*HR II*) is obtained from values of *MCR II* and *HHV*, respectively of the residual coke. It should be noted that the *HHV* of residual coke is calculated according to [49,50]:

$$HHV_{coke} = 19.6\,Y_{coke} + 14.119 \tag{7}$$

where $Y_{coke}$ is the mass fraction of carbon in the coke, which is approximately 0.85 for lignocellulosic biomass coke [51,52]. $HHV_{coke}$ then is approximately 30.80 MJ/kg.

Figure 5 shows the mass loss of OP, $OP_i$, and the standard wood pellets as a function of time. During the ignition interval from 0 to 3 min, the mass decreases slightly. This zone corresponds to the moisture evaporation and to the start of devolatilization. Thereafter, in the main combustion phase, the mass decreases steadily and almost linearly. In this important zone, it is possible to determine the two combustion parameters described above: The mass conversion rate (*MCR I*) and the specific heat release *HR I*. Finally, in the char oxidation zone, the decrease of the mass slows down again. *MCR II* (Figure 5) and *HR II* (Table 6) confirm this observation. The *HR* parameter should be below 1 MW/m$^2$ in the bottom of the bed [23].

The decrease of the heat release rate (*HR II*) in the third zone can be explained by the small oxidation rate of carbon. Moreover, the ignition rates (*IR*) for OP and $OP_i$ are 0.05 (kg/m$^2$)/s and 0.06 (kg/m$^2$)/s, respectively. These values are of the same order of magnitude of the standard wood pellets (0.05 (kg/m$^2$)/s).

**Table 6.** Specification Heat Release in the fuel bed.

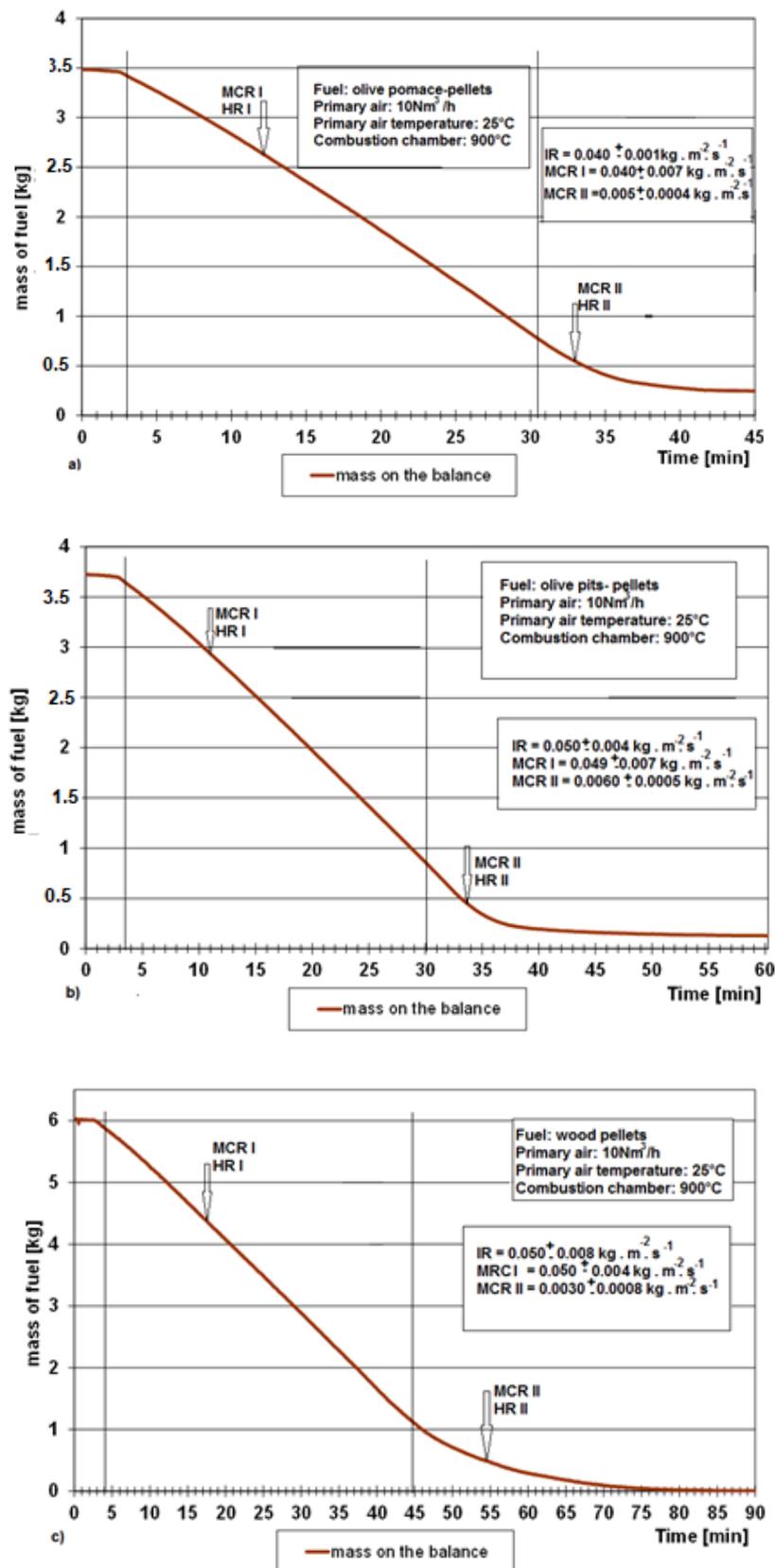| Heat Release | 100% OP | 100% $OP_i$ | Wood Pellets |
|---|---|---|---|
| *HR I* (MW/m$^2$) | $0.96 \pm 0.06$ | $0.98 \pm 0.08$ | $1.01 \pm 0.06$ |
| *HR II* (MW/m$^2$) | $0.12 \pm 0.01$ | $0.12 \pm 0.02$ | $0.070 \pm 0.005$ |

**Figure 5.** Mass loss curves in the fuel bed: (**a**) 100% OP; (**b**) 100% OP$_i$; (**c**) standard wood pellets. Experimental conditions: Primary air 10 Nm$^3$/h; primary air temperature 25 °C, and combustion chamber temperature 900 °C.

*4.3. Gaseous Emissions*

4.3.1. Gaseous Emissions Analysis above the Bed

Figure 6 shows the temporal evolution of the gas concentrations measured directly above the fixed bed (freeboard zone) versus the time during the combustion tests of the different samples. The considered gaseous emissions are respectively; $O_2$, $CO_2$, $H_2O$ (steam), $H_2$, and $C_{org}$ (organic carbon). All components are expressed in % vol. wet basis. Moreover, the local constant of air (λ) is plotted on the right axis.

At the beginning of all experimental tests, only the $O_2$ concentration in the flue gases is detected in the freeboard due to the primary air supply, and then it decays quickly from the ambient level of 21% to zero percent. In contrast, the $H_2O$ mass flow increases due to the fuel bed drying process. After 4 to 5 min, the fuel ignites. Consequently, the concentrations of CO and $CO_2$ increases rapidly, while, $H_2$, $C_{org}$, and $H_2O$ are released. Hence, the concentration of $O_2$ is significantly decreased. In addition, we observe that the gaseous emissions remain at a roughly constant level during the combustion process. This period is called: The main combustion zone or the quasi-stationary combustion zone [23]. During the time interval [37 min, 56 min], the reaction front reaches the bottom of the bed. Consequently, we observe a rise in the $O_2$ concentration again, while the concentrations of $H_2$ and $C_{org}$ are decreased to their minimum levels. During this period, the char residue burning is enhanced exhibiting a little increase of $CO_2$. In contrast, CO rises also steeply with the decrease in $CO_2$ and stabilizes between 20% and 28%. This observation can be attributed to the gasification process for which the residual char is exposed, especially in the presence of $CO_2$ in the medium [21] according to the following reaction:

$$C + CO_2 \rightarrow 2CO \tag{8}$$
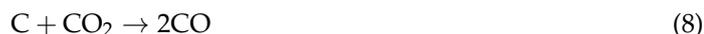
In this zone, the OP pellets are characterized by a high emission of CO which rises to 23% by comparison to 20.2% for the $OP_i$. But, this concentration remains quietly smaller than the 24.5% for the wood pellets. However, during the combustion process, these values remain still higher than those of $CO_2$ emissions. This growth may be attributed to the gasification process of the residual char in the presence of the water/steam ($H_2O$) according to the following reaction:

$$C + H_2O \rightarrow CO + H_2 \tag{9}$$

Indeed, this reaction yields an increase in CO and $H_2$ at the same time [21,53]. Moreover, Figure 6a shows that OP results in the highest percentage of $CO_2$ (≈13%) compared to the 11% for $OP_i$. This result can be attributed to the high percentage of carbon content (about 49.5%) against only 46.5% of the $OP_i$. After a combustion time within the interval from 43 to 70 min, all gaseous emissions tend to zero, indicating the end of fuel conversion process.

Therefore, the comparison of the different samples shows that the wood pellets (Figure 6c) have the most stable emissions compared to OP and $OP_i$. Such behavior may be attributed first, to the lower moisture content (about 6.5%) compared with other samples, and second, to the chemical complexity of OMSWs samples when compared with wood pellets. Indeed, the chemical composition of the olive mill solid wastes is more complex with polyphenols, pectin, and fatty acids. In addition, this difference of behavior between woody pellets and OMSWs pellets can be attributed to the fact that the used reactor was designed to be fed by woody biomass rather than by olive mill by-products. Hence, modifications concerning primary air and secondary air positions and flow rates should be undertaken to increase the reactor efficiency when using OMSWs pellets.
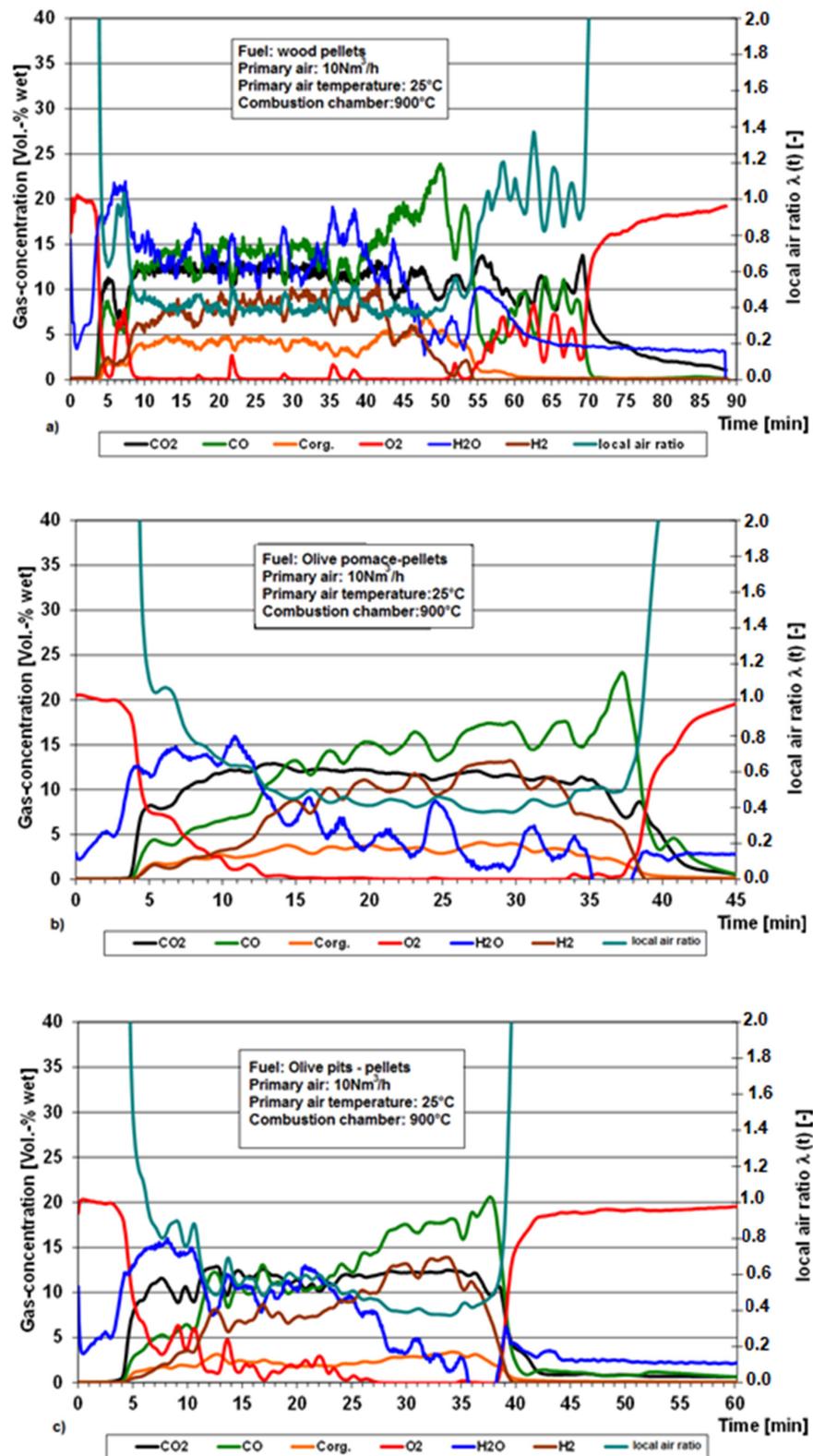
**Figure 6.** Concentrations of gaseous emissions analysis above the fixed bed (in the freeboard): (**a**) 100% standard wood pellets, (**b**) OP and (**c**) 100% OP$_i$. Experimental conditions: Primary air 10 Nm$^3$/h; primary air temperature 25 °C and combustion chamber temperature 900 °C.

4.3.2. Gaseous Emissions Analysis in the Post-Combustion Chamber

Figure 7 shows the temporal distribution of the traces of gas concentrations versus time in the flame front, especially, at the outlet of the post-combustion chamber. More specifically, we focus in this section on $NO_x$ (nitrogen oxides), $N_2O$ (nitrous oxide), and $SO_2$ (sulphur dioxide), expressed in mg/$Nm^3$, dry at normal temperature (25 °C) and pressure. Meanwhile, $O_2$, $CO_2$, and $CO$ concentrations are also considered.
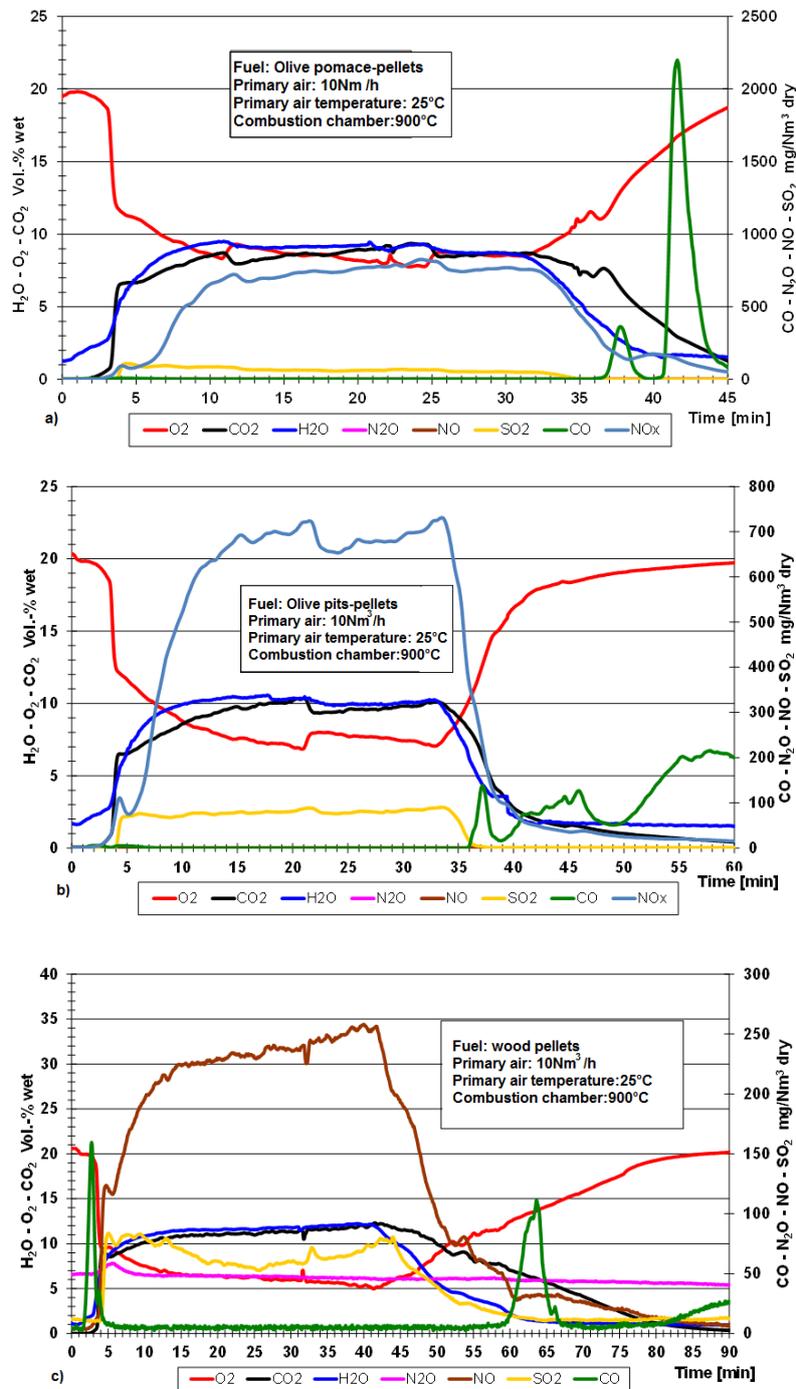


**Figure 7.** Traces of gases measured at the outlet of the post-combustion chamber (**a**) 100% OP; (**b**) 100% $OP_i$ and (**c**) wood pellets.

When examining Figure 7, we observe that the emissions of $NO_x$ at the secondary combustion chamber are relatively high when compared to the $SO_2$ emission. This increase may be attributed to the fuel-N combustion occurring in the post-combustion especially in the presence of a high flow of injected secondary air. Hence, a notable increase of the temperature in the medium results in NO formation (or thermal NO), and the corresponding mechanism is the so-called Zel'dovich mechanism. This mechanism consists of molecules dissociation at high temperature so that each molecule of oxygen and nitrogen in lean flame condition (Equivalence ratio less than 1.0) is dissociated into two atoms. Hence, the pair of reactions was first proposed by Y.B. Zel'dovich [54]:

$$O + N_2 \rightarrow NO + N \tag{10}$$

$$N + O_2 \rightarrow NO + O \tag{11}$$

Furthermore, the reduction of CO is consistent with the increase of the excess air in the secondary combustion chamber [55]. In contrast, Garijo et al. [56] and Staiger et al. [57] indicate that an increase in the CO concentration or another carbonaceous compound can inhibit the formation of $NO_x$. This is mainly due to a reduction of the temperature by heat absorption in the medium. On the other hand, the emissions of $NO_x$ (Figure 7a) of the OP showed the highest value with about 895 mg/Nm$^3$ compared to 720 mg/Nm$^3$ (Figure 7b) of the $OP_i$ and to almost 255 mg/Nm$^3$ (Figure 7c) of the wood pellets. In fact, this result is expected because the nitrogen content in olive pomace (1.26%) is higher than that of wood pellets (0.11%) and also than that of olive pits (0.61%) [58,59]. Moreover, this $NO_x$ concentration growth can also be justified by the abundance of $O_2$ supplied to the post-combustion chamber [28]. In contrast, the emissions of $SO_2$ during the combustion tests of the pellets samples (OP and $OP_i$) exhibit only small traces of this compared to standards biofuels (ex. wood pellets). This may be attributed to the low sulphur contents ($\leq 0.1$) for the different samples.

4.3.3. Conversion Unit of Gaseous Emissions

The gaseous emissions that we obtained were corrected and converted at 10% and 13% $O_2$ according to the following formula:

$$X_{O_2,ref} = X_{O_2,meas} \frac{21 - [O_2]_{ref}}{21 - [O_2]_{meas}} \tag{12}$$

The purpose of this conversion is to allow comparison between our results and those found by authors working under same conditions (10% $O_2$ and 13% $O_2$) and for which gaseous concentrations were expressed either in ppm or in mg/Nm$^3$ as it is summarized in Table 7.

where $X$ is the gas concentration, the subscript "$O_2$, ref" refers to the fixed oxygen concentration under which we want calculate $X$, and the subscript "$O_2$, meas" is related to the measured $X$ value under the fixed oxygen value during the experiment.

We notice that gaseous emissions obtained in our study, with a fixed bed of 40 kW, are in the same range as other lignocellulosic materials. However, the concentrations of nitrogen oxides ($NO_2 + NO$) obtained at the post-combustion chamber were equal to 142 ppm and 116 ppm, at 10% $O_2$ for OP and $OP_i$, respectively. These values are of the same magnitude than 113 ppm $NO_x$ obtained for the standard wood pellets. However, these values are higher than value obtained with the DIN plus (54 ppm at 10% $O_2$) [60]. In fact, the concentrations of $NO_x$ were comparatively smaller (<30 ppm at 13% $O_2$), during the combustion of commercial pine pellets in a domestic pellets boiler (22 kW) [61]. Moreover, these values are close to those found in the literature for various pellets such as exhausted olive mill solid wastes (EOMSW) (115 ppm at 10% $O_2$), and olive pruning pellets (340 ppm at 10% $O_2$) [62]. Furthermore, the values of $SO_2$ varied between 14 and 22 ppm at 10% $O_2$ and between 10 and 16 ppm at 13% $O_2$ according to the obtained results. Nevertheless, these values remain lower than 36 ppm at 10% $O_2$ obtained for Sunflower shells [63]. Mohon et al. [64] showed that the combustion

of grass pellet and three different types of wood pellets, when tested in a prototype pellet furnace (7–32 kW), emit between 0 and 7 ppm of $SO_2$ at 10% $O_2$.

**Table 7.** Emissions values corrected at respectively; (a) 10% $O_2$ and (b) 13% $O_2$.

| Samples | $O_2$% | $CO_2$% | CO [1] % | $H_2O$% | $H_2$% | CO [2] (ppm) | $NO_x$ (ppm) | $SO_2$ (ppm) |
|---|---|---|---|---|---|---|---|---|
| 100 OP | 11 | 6.84 | 11.58 | 8 | 7.63 | (a) 1446 (b) 1054 | (a) 142 (b) 104 | (a) 22 (b) 16 |
| 100 $OP_i$ | 10.37 | 5.85 | 10.64 | 8 | 7.72 | (a) 133 (b) 97 | (a) 116 (b)84 | (a) 17 (b) 12 |
| Wood pellets | 9.94 | 7 | 12.62 | 11.57 | 5.26 | (a) 46 (b) 34 | (a) 13 for $N_2O$; 100 for NO (b) 11 for $N_2O$; 73 for NO | (a) 14 (b) 10 |
| Spent coffee ground (SCG) [65] | 4 | 5 | - | - | - | (a) 2456 (b) 1785 | (a) 245 for NO; 39 for $N_2O$ (b) 178 for NO; 28 for $N_2O$ | - |
| Wood DIN plus [60] | 12 | 6 | - | - | - | (b) 153 | (b) 19 | - |
| EOMSW [36] | 12 | 8 | - | - | - | (a) 795 (b) 578 | (a) 115 (b) 85 | - |
| Sawdust (S) [36] | 12 | 6 | - | - | - | (a) 277 (b) 202 | (a) 36 (b) 26 | - |
| Sunflower shells [61] | 13 | - | - | - | - | (a) 252 | (a) 55 | (a) 36 |
| French Wood pellets [61] | 15 | 6 | - | - | - | (a) 277 | (a) 36 | (a) 7 |
| Pine pellets [62] | 13.22 | 4.5 | - | - | - | (b) 470 | (b) 50 | - |

OMSW: olive mill solid waste, EOMSW: exhaust olive mill solid waste; [1] At the primary combustion chamber; [2] At the post-combustion chamber.

## 5. Conclusions

In this paper, olive pomace OP and olive pits $OP_i$ have been investigated as renewable and environmentally friendly energy sources. More precisely, we focused on the combustion of the pelletized biofuels in a 40 kW counter-current fixed bed reactor. The temperature inside the bed and the mass loss were measured. Three distinct phases for the progress of the combustion process were observed: The ignition delay time, the main combustion phase, and the char oxidation phase. Moreover, some crucial combustion parameters were evaluated: The reaction front velocity, the ignition rate, the heat release rate, and the mass conversion rate.

We have found that the results are quite similar to results of the standard wood pellets which are used currently in European markets. Moreover, we have observed that the gaseous emissions are produced in acceptable concentrations compared to Germany and European standards. Hence, these results motivate future investigations to reuse the olive mill solid wastes for producing alternative biofuels which can be used for heat and/or electricity production, either in domestic or in industrial plants.

## Nomenclature

| | |
|---|---|
| $A$ | Fuel bed cross-section ($m^2$) |
| $HHV$ | Higher heating value ($MJ \cdot kg^{-1}$) |
| $HR$ | Heat release rate ($MW \cdot m^{-2}$) |
| $IR$ | Ignition rate ($kg \cdot m^{-2} \cdot s^{-1}$) |
| $MCR$ | Mass conversion rate ($kg \cdot m^{-2} \cdot s^{-1}$) |
| $h$ | Bed height (mm) |
| $\dot{m}$ | Mass loss rate ($kg \cdot s^{-1}$) |
| $u$ | Velocity ($mm \cdot min^{-1}$) |
| $y$ | Mass fraction (-) |
| $\rho$ | Density ($kg \cdot m^{-3}$) |
| $L$ | Latent heat ($kJ \cdot kg^{-1}$) |

**Subscripts and Superscripts**

| | |
|---|---|
| *ash* | ash |
| *RF* | Reaction front |
| $C_{coke}$ | Carbon in coke |
| *BD* | Bulk density |
| *v* | vaporization |

## References

1. Demirbas, A. Combustion characteristics of different biomass fuels. *Prog. Energy Combust. Sci.* **2004**, *30*, 219–230. [CrossRef]
2. Heschel, W.; Rweyemamu, L.; Scheibner, T.; Meyer, B. Abatement of emission in small-scale combustors through utilization ofblended pellet fuels. *Fuel Process. Technol.* **1999**, *61*, 223–242. [CrossRef]
3. Saidur, R.; Abdelaziz, E.A.; Demirbas, A.; Hossain, M.S.; Mekhilef, S. A review on biomass as a fuel for boilers. *Renew. Sustain. Energy Rev.* **2011**, *15*, 2262–2289. [CrossRef]
4. Christoforou, E.; Fokaides, P.A. A review of olive mill solid wastes to energy utilisation techniques. *Waste Manag.* **2016**, *49*, 346–363. [CrossRef] [PubMed]
5. Rodríguez, G.; Lama, A.; Rodríguez, R.; Jiménez, A.; Guillén, R.; Fernández-Bolaños, J. Olive stone an attractive source of bioactive and valuable compounds. *Bioresour. Technol.* **2008**, *99*, 5261–5269. [CrossRef] [PubMed]
6. Lopez, F.J.; Pinzi, S.; Ruiz, J.J.; Lopez, A.; Dorado, M.P. Economic viability of the use of olive tree pruning as fuel for heating systems in public institutions in South Spain. *Fuel* **2010**, *89*, 1386–1391. [CrossRef]
7. Moya López, A.J.; Mateo Quero, S. Aprovechamiento de los residuos del olivar. Available online: https://www.researchgate.net/publication/259228577_Aprovechamiento_de_los_residuos_del_olivar (accessed on 20 June 2018).
8. Mata-Sánchez, J.; Pérez-Jimenéz, J.A.; Díaz-Villanueva, M.J.; Serrano, A.; Núñez-Sánchez, N.; López-Giménez, F.J. Development of Olive stones quality system based on biofuel energetic parameters study. *Renew. Energy* **2014**, *66*, 251–256. [CrossRef]
9. Pattara, C.; Cappelletti, G.M.; Cichelli, A. Recovery and use of olive stones: commodity, environmental and economic assessment. *Renew. Sustain. Energy Rev.* **2010**, *14*, 1484–1489. [CrossRef]
10. Alkhamis, T.M.; Kablan, M.M. Olive cake as an energy source and catalyst for oil shale production of energy and its impacton the environmental. *Energy Convers. Manag.* **1999**, *40*, 1863–1870. [CrossRef]
11. Ramachandran, S.; Singh, S.K.; Larroche, C.; Soccol, C.R.; Pandey, A. Oil cakes and their biotechnological applications—A reviews. *Bioresour. Technol.* **2007**, *98*, 2000–2009. [CrossRef] [PubMed]
12. Brlek, T.; Pezo, L.; Voća, N.; Krička, T.; Vukmirović, Đ.; Čolović, R.; Bodroža-Solarov, M. Chemometric appraoch for assessing the quality of olive cake pellets. *Fuel Process. Technol.* **2013**, *116*, 250–256. [CrossRef]
13. Christoforou, E.; Kylili, A.; Fokaides, P.A. Technical and economical evaluation of olive mills solid waste pellets. *Renew. Energy* **2016**, *96*, 33–41. [CrossRef]
14. González, J.F.; González-García, C.M.; Ramiro, A.; González, J.; Sabio, E.; Gañán, J.; Rodríguez, M.A. Combustion optimisation of biomass residue pellets for domestic heating with a mural boiler. *Biomass Bioenergy* **2004**, *27*, 145–154. [CrossRef]

15. Lajili, M.; Jeguirim, M.; Kraiem, N.; Limousy, L. Performance of a household boiler fed with agropellets blended from olive mill solid waste and pine sawdust. *Fuel* **2015**, *153*, 431–436. [CrossRef]

16. Miranda, T.; Arranz, J.I.; Montero, I.; Román, S.; Rojas, C.V.; Nogales, S. Characterization and combustion of olive pomace and forest residue pellets. *Fuel Process. Technol.* **2012**, *103*, 91–96. [CrossRef]

17. Miranda, M.T.; Cabanillas, A.; Rojas, S.; Montero, I.; Ruiz, A. Combined combustion of various phases of olive wastes in a conventional combustor. *Fuel* **2007**, *86*, 367–372. [CrossRef]

18. Khodaei, H.; Al-Abdeli, Y.M.; Guzzomi, F.; Yeoh, G.H. An overview of processes and considerations in the modelling of fixed-bed biomass combustion. *Energy* **2015**, *88*, 946–972. [CrossRef]

19. Yang, Y.B.; Sharifi, V.N.; Swithenbank, J. Effect of air flow rate and fuel moisture on the burning behaviours of biomass and simulated municipal solid wastes in packed beds. *Fuel* **2004**, *83*, 1553–1562. [CrossRef]

20. Porteiro, J.; Patiño, D.; Collazo, J.; Granada, E.; Moran, J.; Miguez, J.L. Experimental analysis of the ignition front propagation of several biomass fuels in a fixed-bed combustor. *Fuel* **2010**, *89*, 26–35. [CrossRef]

21. Ménard, Y. Modélisation de L'incinération sur Grille D'ordures Ménagères et Approche Thermodynamique du Comportement des Métaux Lourds. Ph.D. Thesis, National Polytechnic Institute of Lorraine, Nancy, France, July 2008.

22. Mätzing, H.; Germann, H.-J.; Kolb, T.; Seifert, H. Experimental and numerical investigation of wood particle combustion in fixed bed reactors. *Environ. Eng. Sci.* **2012**, *29*, 907–914. [CrossRef]

23. Baris, D.; Gehrmann, H.-J.; Mätzing, H.; Stapf, D.; Seifert, H.; McGowan, T. Characterization of the combustion behavior of "DMC fuel$^{TM}$". In Proceedings of the 34th International Conference on Thermal Treatment Technologies and Hazardous Waste Combustors, Houston, TX, USA, 20–22 October 2015.

24. Demirbas, A. Potential applications of renewable energy sources, biomass combustion problems in boiler power systems and combustion related environmental issues. *Prog. Energy Combust. Sci.* **2005**, *31*, 171–192. [CrossRef]

25. Demirbas, A. Calculation of higher heating values of biomass fuels. *Fuel* **1997**, *76*, 431–434. [CrossRef]

26. McKendry, P. Energy production from biomass (part 1): Overview of biomass. *Bioresour. Technol.* **2002**, *83*, 37–46. [CrossRef]

27. Vassilev, S.V.; Baxter, D.; Andersen, L.K.; Vassileva, C.G. An overview of the chemical composition of biomass. *Fuel* **2010**, *89*, 913–933. [CrossRef]

28. Varol, M.; Atimtay, A.T. Combustion of olive cake and coal in a bubbling fluidized bed with secondary air injection. *Fuel* **2007**, *86*, 1430–1438. [CrossRef]

29. Borello, D.; De Caprariis, B.; DeFilippis, P.; Di Carlo, A.; Marchegiani, A.; Marco Pantaleo, A.; Shah, N.; Venturini, P. Thermo-economic Assessment of a olive pomace Gasifier for Cogeneration Applications. *Energy Procedia* **2015**, *75*, 252–258. [CrossRef]

30. González, J.F.; Román, S.; Encinar, J.M.; Martínez, G. Pyrolysis of various biomass residues and char utilization for the production of activated carbons. *J. Anal. Appl. Pyrolysis* **2009**, *85*, 134–141. [CrossRef]

31. Atimay, A.T. Combustion of agro-waste with coal in fluidized bed. *Clean Technol. Environ. Policy* **2010**, *12*, 43–52. [CrossRef]

32. Abu-Qudais, M. Fluidized bed combustion for energy production from olive cake. *Energy* **1996**, *21*, 173–178. [CrossRef]

33. Skoulou, V.; Koufodimos, G.; Samaras, Z.; Zabaniotou, A. Low temperature gasification of olive kernels in a 5-kW fluidized bed reactor for $H_2$-rich producer gas. *Int. J. Hydrogen Energy* **2008**, *33*, 6515–6524. [CrossRef]

34. Chiang, K.-Y.; Chien, K.-L.; Lu, C.-H. Characterization and comparison of biomass produced from various sources: suggestions for selection of pretreatment technologies in biomass-to-energy. *Appl. Energy* **2012**, *100*, 164–171. [CrossRef]

35. Nunes, L.J.R.; Matias, J.C.O.; Catalão, J.P.S. Mixed biomass pellets for thermal energy production: a review of combustion models. *Appl. Energy* **2014**, *127*, 135–140. [CrossRef]

36. Karkania, V.; Fanara, E.; Zabaniotou, A. Review of sustainable biomass pellets production—A study for agricultural residues pellets' market in greece. *Renew. Sustain. Energy Rev.* **2012**, *16*, 1426–1436. [CrossRef]

37. Lajili, M.; Limousy, L.; Jeguirim, M. Physico-chemical properties and thermal degradation characteristics of agropellets from olive mill by-products/sawdust blends. *Fuel Process. Technol.* **2014**, *126*, 215–221. [CrossRef]

38. Fasina, O.O. Physical properties of peanut hull pellets. *Bioresour. Technol* **2008**, *99*, 1259–1266. [CrossRef] [PubMed]

39. Lehtikangas, P. Quality properties of pelletised sawdust, logging residues and bark. *Biomass Bioenergy* **2001**, *20*, 351–360. [CrossRef]

40. Markovic, M.; Bramer, E.A.; Brem, G. Experimental investigation of wood combustion in a fixed bed with hot air. *Waste Manag.* **2014**, *34*, 49–62. [CrossRef] [PubMed]

41. Kolb, T.; Bleckwehl, S.; Gehrmann, H.-J.; Seifert, H. Characterisation of combustion behaviour of refuse derived fuel. *J. Energy Inst.* **2008**, *81*, 1–6. [CrossRef]

42. Thunman, H.; Leckner, B. Co-current and counter-current fixed bed Combustion of biofuel: A comparison. *Fuel* **2003**, *82*, 275–283. [CrossRef]

43. Porteiro, J.; Patiño, D.; Miguez, J.L.; Granada, E.; Moran, J.; Collazo, J. Study of the reaction front thickness in a counter-current fixed-bed combustor of a pelletised biomass. *Combust. Flame* **2012**, *159*, 1296–1302. [CrossRef]

44. Meranda, T.; Montero, I.; José Sepúlveda, F.; Arranz, J.I.; Rojas, C.V.; Nogales, S. A review of pellets from different sources. *Materials* **2015**, *8*, 1413–1427. [CrossRef] [PubMed]

45. Magelli, F.; Boucher, K.; Bi, H.T.; Melin, S.; Bonoli, A. An environmental impact assessment of exported wood pellets from canada to europe. *Biomass Bioenergy* **2009**, *33*, 434–441. [CrossRef]

46. Ryu, C.; Phan, A.N.; Yang, Y.; Sharifi, V.N.; Swithenbank, J. Ignition and burning rates of segregated waste combustion in packed beds. *Waste Manag.* **2007**, *27*, 802–810. [CrossRef] [PubMed]

47. Gehrmann, H.-J.; Kolb, T.; Seifert, H.; Mark, F.E.; Frankenhaeuser, M.; Schanssema, A.; Wittstock, K.; Kolb, J.J. Synergies between biomass and solid recovered fuel in energy conversion processes. *Environ. Eng. Sci.* **2010**, *27*, 557–567. [CrossRef]

48. Shin, D.; Choi, S. The combustion of simulated waste in a fixed bed. *Combust. Flame* **2000**, *180*, 121–167. [CrossRef]

49. Ahmaruzzaman, M. Proximate analyses and predicting hhv of chars obtained from cocracking of petroleum vacuum residue with coal, plastics and biomass. *Bioresour. Technol.* **2008**, *99*, 5043–5050. [CrossRef] [PubMed]

50. Vargas-Moreno, J.M.; Callejón-Ferre, A.J.; Pérez-Alonso, J.; Velázquez-Martí, B. A review of the mathematical models for predicting the heating value of biomass materials. *Renew. Sustain. Energy Rev.* **2012**, *16*, 3065–3083. [CrossRef]

51. Kawakami, M.; Karato, T.; Takenaka, T.; Yokoyama, S. Structure analysis of coke, wood charcoal and bamboocharcoal by Raman spectroscopy and the irreaction rate with $CO_2$. *ISIJ Int.* **2005**, *45*, 1027–1034. [CrossRef]

52. Mueller, A.; Haustein, H.D.; Stoesser, P.; Kreitzberg, T.; Kneer, R.; Kolb, T. Gasification kinetics of biomass- and fossil-based fuels: Comparison study using fluidized bed and thermogravimetric analysis. *Energy Fuels* **2015**, *29*, 6717–6723. [CrossRef]

53. Imen, G.; Mejdi, J.; Uta, S.; Lionel, L.; Simona, B.; Eckhard, D.; Christof, A.; Roman, L.; Frank, S.; Abedlmottaleb, O. The Potential of Activated Carbone Made From Agro-Industrial Residues in $NO_x$ Immessions. *Energies* **2017**, *10*, 1508. [CrossRef]

54. Anetor, L.; Odetunde, C.; Osakue, E.E. Computational Analysis of Extended Zel'dovich Mechanism. *Arab. J. Sci. Eng.* **2014**, *39*, 8287–8305. [CrossRef]

55. Atimtay, A.T.; Varol, M. Investigations of co-combustion of coal and olive cake in a bubbling fluidized bed with secondary air injection. *Fuel* **2009**, *88*, 1000–1008. [CrossRef]

56. Garijo, E.G.; Jensen, A.D.; Glarborg, P. Kinetic Study of NO Reduction over Biomass Char under Dynamic Conditions. *Energy Fuels* **2003**, *17*, 1429–1436. [CrossRef]

57. Staiger, B.; Unterberger, S.; Berger, R.; Hein, K.R.G. Development of an air staging technology to reduce NOx emissions in grate-fired boilers. *Energy* **2005**, *30*, 1429–1438. [CrossRef]

58. Nussbaumer, T. Combustion and co-combustion of biomass: Fundamentals, Technologies and Primary measures for Emission Reduction. *Energy Fuels* **2003**, *15*, 10–21. [CrossRef]

59. Stubenberger, G.; Scharler, R.; Zahirovic, S.; Obernberger, I. Experimental investigation of nitrogen species release from different solid biomass fuels as basis for release models. *Fuel* **2008**, *87*, 793–806. [CrossRef]

60. Kraiem, N.; Lajili, M.; Limousy, L.; Said, R.; Jeguirim, M. Energy recovery from Tunisian agri-food wastes: Evaluation of combustion performance and emissions characteristics of green pellets prepared from tomato residues and grape marc. *Energy* **2016**, *107*, 409–418. [CrossRef]

61. Fernandes, U.; Costa, M. Particle emissions from a domestic pellets-fired boiler. In Proceedings of the 4th International Congress on Energy and Environment Engineering and Management, Mérida, Spain, 26–27 May 2011.

62. Garcia-Maraver, A.; Zamorano, M.; Fernandes, U.; Rabaçal, M.; Costa, M. Relationship between fuel quality and gaseous and particulate matter emission in a domestic pellet-fired boiler. *Fuel* **2014**, *119*, 141–152. [CrossRef]

63. Cardozo, E.; Erlich, C.; Alejo, L.; Fransson, T.H. Combustion of agriculture residues: An experimental study for small-scale applications. *Fuel* **2014**, *115*, 778–787. [CrossRef]

64. Roy, M.M.; Dutta, A.; Corscadden, K. An experimental study of combustion and emissions of biomass pellets in a prototype pellet furnace. *Appl. Energy* **2013**, *108*, 298–307. [CrossRef]

65. Limousy, L.; Jeguirim, M.; Dutournié, P.; Kraiem, N.; Lajili, M.; Said, R. Gaseous products and particulate matter emissions of biomass residual boiler fired with spent coffee ground pellets. *Fuel* **2013**, *107*, 323–329. [CrossRef]